Microchimica Acta (2018) 185: 17
https://doi.org/10.1007/s00604-017-2541-4

ORIGINAL PAPER

Inner filter effect based fluorometric determination of the activity of alkaline phosphatase by using carbon dots codoped with boron and nitrogen

Mi Mao[1] · Tian Tian[1] · Yu He[1,2,3] · Yili Ge[1,2] · Jiangang Zhou[3] · Gongwu Song[1,2]

Received: 13 July 2017 / Accepted: 9 November 2017 / Published online: 5 December 2017

Abstracts

Boron and nitrogen codoped carbon dots functionalized with cyclodextrin (β-CD-N/B-C-dots) were obtained from β-cyclodextrin. The material displays strong fluorescence (with excitation/emission peak wavelengths of 400/500 nm) and was characterized by UV-vis, transmission electron microscopy and FTIR. If the substrate p-nitrophenylphosphate is enzymatically cleaved by alkaline phosphatase (ALP), a yellow product is formed whose absorption overlaps the excitation spectrum of the β-CD-N/B-C-dots. Hence, fluorescence is reduced due to an inner filter effect. In additon, the β-CD cavity offers a pocket for substrate recognition. The findings were used to design a method for the determination of the activity of ALP. It has a working range that extends from 0.003 to 5.5 $U{\cdot}L^{-1}$, with a 0.3 $mU{\cdot}L^{-1}$ detection limit. The method is fast, simple, inexpensive, and highly sensitive and selective.

Keywords Enyzyme activity assay · Host-guest recognition · β-Cyclodextrin · N/B-C-dots · Fluorescence · Host-guest recognition

Introduction

Alkaline phosphatase (ALP) is an essential enzyme in phosphate metabolism to catalyze the dephosphorylation process of nucleic acids, proteins, and some small molecules [1–4]. As the most common human alkaline phosphatase, ALP has been identified as an important biomarker in the diagnosis of many diseases. The abnormal level of ALP in serum is closely related to various diseases such as breast and prostatic cancer [5, 6], bone disease [7], liver dysfunction and diabetes [8, 9]. Therefore, significant efforts have been devoted to explore new method for the detection of ALP.A number of technologies have been employed for the detection of ALP, such as colorimetry [10–12], surface enhanced resonance Raman scattering [13, 14], fluorescence [15–17], electrochemistry [18]. Because of its fast analysis and high sensitivity, fluorescence method had become a hot topic for the detection of ALP owing to their high sensitivity, cost–effectiveness, simplicity, and convenience. Many fluorescent chemosensors have been successfully applied to detect ALP activity based on organic fluorescent dyes [19, 20], conjugated polyelectrolytes [21, 22], and inorganic semiconductor quantum dots (QDs) [23, 24]. However, organic dyes and QDs in practical applications can be limited by relative poor photostability (for organic fluorophores) or toxicity (e.g.QDs). There is a need to develop sensitive, simple and non-toxic methods for ALP activity monitoring.

Carbon dots (C-dots), one of the C-based materials, are superior to quantum dots and organic dyes in terms of excellent physicochemical and photochemical properties, good biocompatibility, low toxicity and easy to preparation [25–29]. B and N, the neighboring elements of carbon (C) in the periodic table, have atomic radii similar to C, which make it possible to efficiently modulate the properties of C-dots after doping.

Electronic supplementary material The online version of this article (https://doi.org/10.1007/s00604-017-2541-4) contains supplementary material, which is available to authorized users.

✉ Yu He
heyu@hubu.edu.cn

[1] Hubei Collaborative Innovation Center for Advanced Organic Chemical Materials, Wuhan 430062, China

[2] Ministry-of-Education Key Laboratory for the Synthesis and Application of Organic Functional Molecules, College of Chemistry and Chemical Engineering, Hubei University, Wuhan 430062, China

[3] Hubei Province Key Laboratory of Regional Development and Environment Response, Wuhan 430062, China

Most of previous methods introduce two or more compounds as the starting materials to synthesize B and N doped C-dots. Single starting material to synthesize B and N co-doped C-dots, containing B and N simultaneously, can simplify the synthesis process and reduce the byproducts [30]. β-Cyclodextrin (β-CD) can form host-guest complexes with a wide range of hydrophobic guest species through noncovalent interactions [31]. Previous works reported β-cyclodextrin serve as a modulator to greatly improve the catalytical activity of nanomaterial, because they can form complexes with hydrophobic compounds to offer a pocket for the substrate recognition [32–34]. However, there are only limited work focusing on the synthesis and application of β-cyclodextrin based C-dots [35–40].

Herein, we introduce 3-aminophenylboronic acid (APBA) as starting material to fabricate B and N co-doped carbon dots (N/B-C-dots) with high quantum yield through one-pot hydrothermal method without further passivation. Then, we synthesized the cyclodextrin functionalized B and N co-doped carbon dots (β-CD-N/B-C-dots) using mono-6-thio-β-CD as modifier and N/B-C-dots as precursors. With the aid of β-CD, the detection performance of N/B- C-dots is excellent because the cavity of β-CD offered a pocket for substrate recognition (Scheme 1). Mono-6-thio-β-CD was directly introduced on the surfaces of the N/B-C-dots for ALP activity through host-guest recognition. The p-nitrophenylphosphate (PNPP) as a common substrate in colorimetric determination of ALP was employed as the ALP substrate in this sensing system. The maximum absorption wavelength of its ALP reaction products (p-nitrophenol, PNP) can well overlap with excitation spectra of the N/B-C-dots, leading to the efficient quenching of N/B-C-dots because of the inner filter effect (IEF). The method shows many merits including rapidity, low cost, high sensitivity, and excellent selectivity, providing a new insight on the application of N/B-C-dots to develop the facile and sensitive biometric technology.

Materials and methods

Reagents and chemicals

APBA, alkaline phosphatase, p-nitrophenylphosphate (PNPP), p-nitrophenol (PNP), Thrombin, glucose oxidase (GOx) and p-nitrophenylphosphate were purchased from Aladdin Chemical Co., Ltd. (Shanghai, China, http://aladdin.company.lookchem.cn/). Mono-6-SH-β-CD was purchased from Shandong Binzhou Zhiyuan Bio-Technology Co., Ltd. (Shandong, China, http://www.bzzysw.com). Sodium hydroxide (NaOH), ascorbic acid (AA), cysteine (Cys), glutathione (GSH), lysine (Lys), tryptophan (Try) and glycine (Gly) were purchased from Sinopharm Chemical Reagent Co., Ltd. (Shanghai, China, http://www.shreagent.lookchem.com).

Preparation of N/B-dots

The N/B-dots were synthesized by a hydrothermal method [28]. In a typically experimental procedure, 0.1 g of APBA was dissolved in 10 mL ultrapure water, followed by adding 0.2 mL of 0.1 M NaOH under stirring. Then, the clear and homogeneous solution was transferred into the Teflon-lined autoclave chamber and heated to 180 °C for 4 h. After cooling down to room temperature, the solution was centrifuged at 10000 rpm (5595 rcf) for 10 min to remove large precipitates. The final purified N/B-dots were stored at 4 °C for further use.

Preparation of β-CD-N/B-C-dots

Typically, 0.5 mL of prepared N/B-C-dots was diluted to 5 mL, and then 50 μL of 2 M NaOH and 11.35 mg 6-SH-β-CD were added and homogenized by stirring. The mixture was heated at 70 °C for 4 h. The final solution was stored at 4 °C in refrigerator for use in the next step.

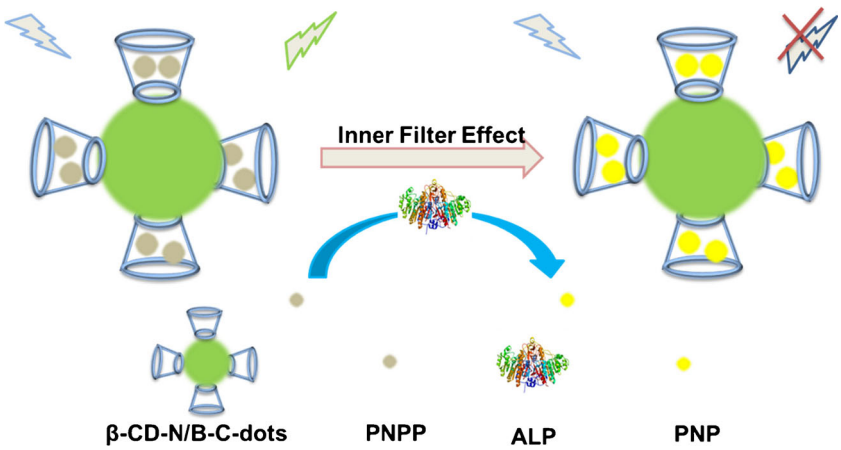

Scheme 1 Mechanism of the assay

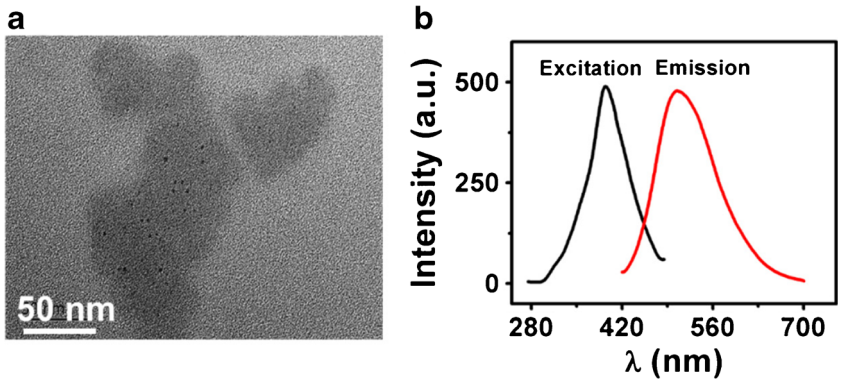

Fig. 1 **a** TEM images of the β-CD-N/B-C-dots, **b** Fluorescence excitation and emission spectra of the β-CD-N/B-C-dots

Characterizations of β-CD-N/B-C-dots

Transmission electron microscopy (TEM) images were obtained on a Tecnai G20 microscope (FEI, America). Fourier-transform infrared (FT-IR) spectra were recorded on FT-IR spectrophotometer (Perkin Elmer, America). UV–vis absorption spectra (UV–vis) were performed on Lamber35 UV spectrometer (Perkin Elmer, America). The fluorescence measurements were recorded on LS55 fluorescence spectrometer (Perkin Elmer, America).

IFE-based fluorometric determination of ALP

The IFE based fluorescent ALP activity assay was performed under the following procedures. A total of 10 μL of ALP with activities from 0 to 114 $U{\cdot}L^{-1}$ (or 10 μL of serum sample) was added into the reaction system (Tris-HCl, pH =8.0), which consisted of 80 μM PNPP and 0.1 μM $MgSO_4$. The reaction solution was incubated at 37 °C for 20 min, after that the mixture was transferred to 1 mL of C-dots solution and then subjected to fluorescence spectral measurements at the excitation wavelength of 400 nm.

Results and discussions

Synthesis and characterization of β-CD-N/B-C-dots

The N/B-C-dots were synthesized by a hydrothermal method [28]. We selected the APBA as the nitrogen and boron-containing starting material for the synthesis of N/B-C-dots. Then, we synthesized the cyclodextrin functionalized B and N co-doped carbon dots (β-CD-N/B-C-dots) using mono-6-thio-β-CD as modifier and N/B-C-dots as precursors. To obtain the optimal synthetic conditions, the influence of reactants concentrations including NaOH and CD, reaction time, and reaction temperature on the fluorescence intensity of mono-6-thio-β-CD modificated N/B-C-dots (β-CD-N/B-C-dots) were investigated, respectively (Fig. S1). Typically, 0.5 mL of prepared β-CD-N/B-C-dots was diluted to 5 mL, and then 50 μL of 2 M NaOH and 11.35 mg 6-SH-β-CD were added and homogenized by stirring. The mixture was heated at 70 °C for 4 h. The final solution was stored at 4 °C in refrigerator for use in the next step.

The morphological structure of β-CD-N/B-C-dots characterized by TEM is displayed at Fig. 1a. The TEM image demonstrates that the β-CD-N/B-C-dots shows well-dispersed without obvious aggregation with the average size is 5 nm.

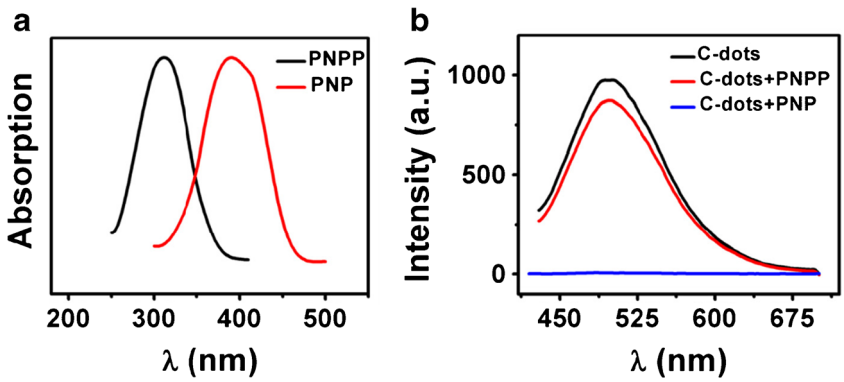

Fig. 2 **a** UV-vis absorption spectra of PNPP and PNP solutions under alkaline conditions, **b** Fluorescence spectra of the β-CD-N/B-C-dots in the presence of PNPP and PNP (excitation peaks at 400 nm)

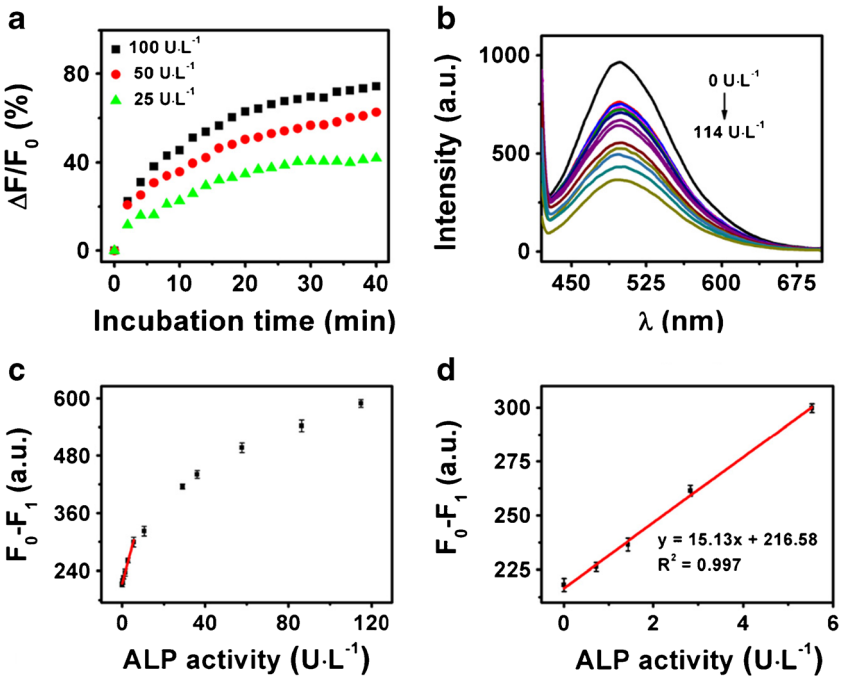

Fig. 3 **a** The relationship between incubation time and quenching efficiency in different concentration of ALP, **b** Fluorescence spectra of β-CD-N/B-C-dots with ALP (0–114 $U{\cdot}L^{-1}$), **c** The plot of fluorescence responses of β-CD-N/B-C-dots (excitation/emission peaks at 400/500 nm), **d** Fluorescence response of β-CD-N/B-C-dots against the concentration of ALP from 0.003 to 5.5 $U{\cdot}L^{-1}$ (excitation/emission peaks at 400/500 nm)

The fluorescence spectra indicate that the optimal excitation and emission wavelengths of β-CD-N/B-C-dots are 400 nm and 500 nm, respectively (Fig. 1b). As shown in Fig. S2 a, the strong peak of 235 nm is ascribed to n → π* transition of C = C-N, and the peak of 290 nm is attributed to π → π* transition of C = C bond. The surface composition of the β-CD-N/B-C-dots is investigated in Fig. S2 b, the peak at 3375 cm^{-1}, 1621 cm^{-1} and 1372 cm^{-1} in the FTIR curve of N/B-C-dots are shifted to 3391 cm^{-1}, 1653 cm^{-1} and 1405 cm^{-1} after the modification of β-CD, demonstrating the formation of β-CD-N/B-C-dots.

Principle of ALP activity assay based on IFE

Introduction of heteroatoms into carbon nanomaterials has been explored to tune the conduction/valence band position of doped carbon material resulting in altered functions. For this purpose, nitrogen was widely used as electron donors, whereas boron was used as an electron acceptor. It is confirmed through various reports that excitons of carbon, emissive traps on C-dots, the quantum confinement effect, aromatic moieties, oxygen contacting groups, free zigzag sites, and edge defects contribute to the fluorescence. In addition to this, we also believe that N-doping as well as B doping also remarkably enhance the fluorescence of C-dots. In this study, PNPP was employed as the substrate of ALP to indirectly determine the activity of ALP based on IFE. IFE phenomenon is due to the absorption of the excitation or emission by absorbers in the detection system when the absorption spectra of the absorbers overlap with the excitation or emission spectra of fluorophores. As shown in Fig. 2a, the maximum UV-vis absorbance of PNPP (300 nm) has no effect on fluorescence intensity of β-CD-N/B-C-dots (500 nm) and the PNPP hydrolysis product (PNP) by ALP has a great molar absorptivity at 400 nm, which has a good overlap with the excitation spectrum of β-CD-N/B-C-dots. To further confirm the feasibility of our design for ALP detection, we recorded the fluorescence spectra of β-CD-N/B-C-dots mixed with PNPP and PNP (excitation peaks at 400 nm). As we expected, the addition of PNP (0.5 mM) quenches the fluorescence intensity of β-CD-N/B-C-dots at 500 nm significantly, while the same addition of PNPP quenches a little (Fig. 2b).

IFE-based fluorescence assay for ALP activity

To obtain the optimum reaction conditions for ALP activity detection, the incubation time was chosen for investigation.

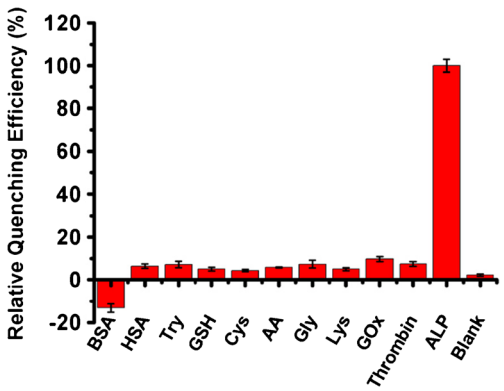

Fig. 4 Selectivity of β-CD-N/B-C-dots to different substances: 50 $mg{\cdot}L^{-1}$ BSA and HSA, 0.1 mM Try, Lys, Cys, Gly, AA and GSH, 10 $U{\cdot}L^{-1}$ Gox, thrombin and ALP

As shown in Fig. 3a, the incubation time for quenching efficiency reaching the maximum are both about 20 min though in different concentration of ALP (25, 50 and 100 $U{\cdot}L^{-1}$). Then we measured ALP activity at the best incubation time. In Fig. 3b, with the increasing of ALP activity, the fluorescence intensity of β-CD-N/B-C-dots probe decreases continuously. A good fitted regression line between the relative fluorescence intensity (F_0 - F) and ALP concentrations is obtained in the range of 0.003 to 5.5 $U{\cdot}L^{-1}$ (Fig. 3c–3d), with a linear regression equation as $Y = 15.13X + 216.58$ ($R^2 = 0.997$). The detecting platform provides an ultralow detection limit of 0.0003 $U{\cdot}L^{-1}$. The performance of the β-CD-N/B-C-dots based assay is compared with literature reported fluorescence assay towards ALP. From Table S1, we can see the performance of our assay was better than literature report. In addition, compared with previous work by You's group [41], because of the introduction of β-CD, the wider and more polar β-CD secondary faces are exposed to bind suitable guest species such as PNPP in the β-CD annulus and in close proximity to the catalytic surface [42] and thereby enhance the probability of catalytic oxidation of PNPP by β-CD-N/B-C-dots.

Selectivity of the method

To evaluate the specificity of the IFE-based assay for ALP, several potential interfering compounds were investigated under the same conditions. 10 μL of various small molecules including 50 $mg{\cdot}L^{-1}$ BSA and HSA, 0.1 mM Try, Lys, Cys, Gly, AA and GSH, 10 $U{\cdot}L^{-1}$ Gox, thrombin and ALP was added into β-CD-N/B-C-dots (dilution with Tris-HCl) with Mg^{2+} (0.1 μM) ion and PNPP (80 μM). After incubated for 20 min at 37 °C, the fluorescence spectrum was recorded under 400 nm excitation. As shown in Fig. 4, at the same class of concentration, all the other small molecules can not significantly affect the fluorescence signals of the β-CD-N/B-C-dots while ALP has an almost 100% quenching effect on the fluorescence intensity of β-CD-N/B-C-dots, indicating the excellent selectivity and applicability of the detecting strategy.

Conclusion

We demonstrate a simple approach to synthesize N/B-C-dots by one-pot hydrothermal method and further obtain β-CD-N/B-C-dots modified fluorescent probe by using mono-6-thio-β-CD as modifier. This modified fluorescent probe was developed for the specific recognition and quantitative detection of ALP in a cost-effective and time-saving way based on the inner filter effect (IFE) of N/B-C-dots. Besides, mono-6-thio-β-CD was directly introduced on the surfaces of the N/B-C-dots for ALP activity through host-guest recognition to improve the sensitivity of the detection system. We believe that this method paves the way for the further exploration and practical application in bioanalysis fields.

Acknowledgements This work was financially supported by Supported by National Natural Science Foundation of China (21707030) and Wuhan Youth Science and technology plan (2016070204010133).

Compliance with ethical standards The author(s) declare that they have no competing interests.

References

1. Harris H (1990) The human alkaline phosphatases: what we know and what we don't know. Clin Chim Acta 186:133
2. Coleman JE (1992) Structure and mechanism of alkaline phosphatase. Annu Rev Biophys Biomol Struct 21:441
3. Fernley H (1971) 18 mammalian alkaline phosphatases. Enzyme 4: 417
4. Zhao MM, Guo YJ, Wang LX, Luo F, Lin CY, Lin ZY, Chen GN (2016) A sensitive fluorescence biosensor for alkaline phosphatase activity based on the Cu(II)-dependent DNAzyme. Anal Chim Acta 948:98
5. Lorente JA, Valenzuela H, Morote J, Gelabert A (1999) Serum bone alkaline phosphatase levels enhance the clinical utility of prostate specific antigen in the staging of newly diagnosed prostate cancer patients. Eur J Nucl Med 26:625
6. Bricon TL, Gay-Bellile C, Cottu P, Benlakehal M, Guillon H, Houze P (2010) Lectin affinity electrophoresis of serum alkaline phosphatase in metastasized breast cancer. J Clin Lab Anal 24:20
7. Miller PD (2014) Bone disease in CKD: a focus on osteoporosis diagnosis and management. Am J Kidney Dis 64:290
8. Limdi JK, Hyde GM (2003) Evaluation of abnormal liver function tests. Postgrad Med J 79:307
9. Lassenius MI, Fogarty CL, Blaut M, Haimila K, Riittinen L, Paju A, Kirveskari J (2017) Intestinal alkaline phosphatase at the crossroad of intestinal health and disease - a putative role in type 1 diabetes. J Intern Med 281:586
10. Yang JJ, Zheng L, Wang Y, Li W, Zhang JL, JJ G, Fu Y (2016) Guanine-rich DNA-based peroxidase mimetics for colorimetric assays of alkaline phosphatase. Biosens Bioelectron 77:549
11. Hu Q, Zhou BJ, Dang PY, Li LZ, Kong JM, Zhang XJ (2017) Facile colorimetric assay of alkaline phosphatase activity using Fe(II)-phenanthroline reporter. Anal Chim Acta 950:170
12. Hu Q, He MH, Mei YQ, Feng WJ, Jing S, Kong JM, Zhang XJ (2017) Sensitive and selective colorimetric assay of alkaline phosphatase activity with Cu(II)-phenanthroline complex. Talanta 163: 146
13. Ingram A, Moore BD, Graham D (2009) Simultaneous detection of alkaline phosphatase and β-galactosidase activity using SERRS. Bioorg Med Chem Lett 19:1569
14. Ruan CM, Wang W, BH G (2006) Detection of alkaline phosphatase using surface-enhanced Raman spectroscopy. Anal Chem 78: 3379
15. Xiang MH, Liu JW, Li N, Tang H, RQ Y, Jiang JH (2016) A fluorescent graphitic carbon nitride nanosheet biosensor for highly sensitive, label-free detection of alkaline phosphatase. Nano 8:4727
16. Deng J, Yu P, Wang Y, Mao L (2015) Real-time ratiometric fluorescent assay for alkaline phosphatase activity with stimulus responsive infinite coordination polymer nanoparticles. Anal Chem 87:3080
17. Kong RM, Fu T, Sun NN, FL Q, Zhang SF, Zhang XB (2013) Pyrophosphate-regulated Zn^{2+}-dependent DNAzyme activity: an

amplified fluorescence sensing strategy for alkaline phosphatase. Biosens Bioelectron 50:351
18. Zhang L, Hou T, Li H, Li F (2015) A highly sensitive homogeneous electrochemical assay for alkaline phosphatase activity based on single molecular beaconinitiated T7 exonuclease-mediated signal amplification. Analyst 140:4030
19. Zhang HM, CL X, Liu J, Li XH, Guo L, Li XM (2015) An enzyme-Activatable probe with a self-Immolative linker for rapid and sensitive alkaline phosphatase detection and cell imaging through a Cascade reaction. Chem Commun 51:7031
20. Chen J, Jiao HP, Li WY, Liao DL, Zhou HP, Yu C (2013) Real-time fluorescence turn-on detection of alkaline phosphatase activity with a novel Perylene probe. Chem-Asian J 8:276
21. Liu Y, Schanze KS (2008) Conjugated polyelectrolyte-based real-time fluorescence assay for alkaline phosphatase with pyrophosphate as substrate. Anal Chem 80:8605
22. Liu H, Lv ZL, Ding KG, Liu XL, Yuan L, Chen H, Li XM (2013) Incorporation of tyrosine phosphate into tetraphenylethylene affords an amphiphilic molecule for alkaline phosphatase detection, hydrogelation and calcium mineralization. J Mater Chem B 1:5550
23. Liu SY, Pang S, Na WD, XG S (2014) Near-infrared fluorescence probe for the determination of alkaline phosphatase. Biosens Bioelectron 55:249
24. Jia L, JP X, Li D, Pang SP, Fang YA, Song ZG, Ji JA (2010) Fluorescence detection of alkaline phosphatase activity with Beta-Cyclodextrin-modified quantum dots. Chem Commun 46:7166
25. Lim SY, Shen W, Gao ZQ (2015) Carbon quantum dots and their applications. Chem Soc Rev 449:362
26. Zheng XT, Ananthanarayanan A, Luo KQ, Chen P (2015) Glowing graphene quantum dots and carbon dots: properties, syntheses, and biological applications. Small 11:1620
27. Zhu SJ, Song YB, Zhao XH, Shao JR, Zhang JH, Yang B (2015) The photoluminescence mechanism in carbon dots (graphene quantum dots, carbon nanodots, and polymer dots): current state and future perspective. Nano Res 8:355
28. Yang Y, Zhang JC, Zhuang J, Wang X (2015) Synthesis of nitrogen-doped carbon nanostructures from polyurethane sponge for bioimaging and catalysis. Nano 7:12284
29. Hu C, Yu C, Li MY, Wang XN, Yang JY, Zhao ZB, Eychmuller A, Sun YP, Qiu JS (2014) Chemically tailoring coal to fluorescent carbon dots with tuned size and their capacity for Cu(II) detection. Small 10:4926
30. Tian T, He Y, Ge YL, Song GW (2017) One-pot synthesis of boron and nitrogen co-doped carbon dots as the fluorescence probe for dopamine based on the redox reaction between Cr(VI) and dopamine. Sensors Actuators B Chem 240:1265
31. Wenz G, Han BH, Muller A (2006) Cyclodextrin rotaxanes and polyrotaxanes. Chem Rev 106:782
32. Zhao XH, Liu X, Lu M (2014) β-cyclodextrin-capped palladium nanoparticle-catalyzed ligand-free Suzuki and Heck couplings in low-melting β-cyclodextrin/NMU mixtures. Appl Organomet Chem 28:635
33. Putta C, Sharavath V, Sarkar S, Ghosh S (2014) Palladium nanoparticles on β-cyclodextrin functionalised graphene nanosheets: a supramolecular based heterogeneous catalyst for C–C coupling reactions under green reaction conditions. RSC Adv 5:6652
34. Chen S, Zhang JB, Gan N, FT H, Li TH, Cao YT, Pan DD (2015) An on-site immunosensor for ractopamine based on a personal glucosemeter and using magnetic β-cyclodextrin-coated nanoparticles for enrichment, and an invertase-labeled nanogold probe for signal amplification. Microchim Acta 182:815
35. Tang C, Qian ZS, Huang YY, JM X, Ao H, Zhao MZ, Zhou J, Chen JR, Feng H (2016) A fluorometric assay for alkaline phosphatase activity based on β-cyclodextrin-modified carbon quantum dots through host-guest recognition. Biosens Bioelectron 83:274
36. Liu H, Ma C, Wang J, Wang K, Wu K (2017) A turn-on fluorescent method for determination of the activity of alkaline phosphatase based on dsDNA-templated copper nanoparticles and exonuclease based amplification. Microchim Acta 184:2483
37. Kang W, Ding Y, Zhou H, Liao Q, Yang X, Yang Y, Yang M (2015) Monitoring the activity and inhibition of alkaline phosphatase via quenching and restoration of the fluorescence of carbon dots. Microchim Acta 182:1161
38. Guo L, Chen D, Yang M (2017) DNA-templated silver nanoclusters for fluorometric determination of the activity and inhibition of alkaline phosphatase. Microchim Acta 184:2165
39. Liu XG, Xing XJ, Li B, Guo YM, Zhang YZ, Yang Y, Zhang LF (2016) Fluorescent assay for alkaline phosphatase activity based on graphene oxide integrating with λ exonuclease. Biosens Bioelectron 81:460
40. Wang Y, Chen J, Jiao H, Chen Y, Li W, Zhang Q, Yu C (2013) Polymer templated perylene-probe noncovalent self-assembly: a new strategy for label-free ultrasensitive fluorescence turn-on biosensing. Chem Eur J 19:12846
41. Li GL, HL F, Chen XJ, Gong PW, Chen G, Xia L, Wang H, You JM, YN W (2016) Facile and sensitive fluorescence sensing of alkaline phosphatase activity with photoluminescent carbon dots based on inner filter effect. Anal Chem 88:2720
42. Liu JJ, Wang J, Zhu ZM, Li L, Guo XH (2014) Cooperative catalytic activity of Cyclodextrin and ag nanoparticles immobilized on spherical polyelectrolyte brushes. AICHE J 60:1977